Appendix 3

MF-Tire/MF-Swift Parameters and Estimation Methods

Igo Besselink

This appendix starts with a complete listing of the tire model parameters of a passenger car tire, which is closely linked to the TNO *MF-Tire/MF-Swift* 6.1 model. The tests required to obtain these parameters are discussed briefly. Furthermore, parameter estimation methods are presented in case no or limited measurement data are available. This is important as, for some classes of tires (e.g. aircraft and truck tires), dedicated measurement equipment may either simply not be available or not suited to handle very large tires.

Table A3.1 gives a listing of the various tire model parameters. Typically, this data is stored in a so-called 'tire property file', which normally has the filename extension '.tir' or '.tpf'. Please note that the ISO sign convention is used.

TABLE A3.1 TNO MF-Tire/MF-Swift 6.1 Tire Model Parameters

Tire Designation: 205/60R15 91 V
[model] $V_o = 16.7$ m/s, $V_{x,\mathrm{low}} = 1$ m/s
[dimension] $r_o = 0.3135$ m, $w = 0.205$ m, $r_{\mathrm{rim}} = 0.1905$ m
[operating_conditions] $p_{io} = 220{,}000$ Pa
[inertia] $m_{\mathrm{tire}} = 9.3$ kg, $I_{xx,\mathrm{tire}} = 0.391$ kg m^2, $I_{yy,\mathrm{tire}} = 0.736$ kg m^2 $m_{\mathrm{belt}} = 7.247$ kg, $I_{xx,\mathrm{belt}} = 0.3519$ kg m^2, $I_{yy,\mathrm{belt}} = 0.5698$ kg m^2

(*Continued*)

TABLE A3.1 TNO MF-Tire/MF-Swift 6.1 Tire Model Parameters—Cont'd

Tire Designation: 205/60R15 91 V

[vertical]
$F_{zo} = 4000$ N
$c_{zo} = 209651$ N/m, $k_z = 50$ Ns/m, $q_{V2} = 0.04667$, $q_{Fz2} = 15.4$, $q_{Fcx} = 0$, $q_{Fcy} = 0$,
$p_{Fz1} = 0.7098$
$B_{\text{reff}} = 8.386$, $D_{\text{reff}} = 0.25826$, $F_{\text{reff}} = 0.07394$, $q_{reo} = 0.9974$, $q_{V1} = 7.742 \cdot 10^{-4}$

[structural]
$c_{xo} = 358066$ N/m, $p_{cfx1} = 0.17504$, $p_{cfx2} = 0$, $p_{cfx3} = 0$
$c_{yo} = 102673$ N/m, $p_{cfy1} = 0.16365$, $p_{cfy2} = 0$, $p_{cfy3} = 0.24993$
$c_{\psi} = 4795$ Nm/rad, $p_{cmz1} = 0$
$f_{\text{long}} = 77.17$ Hz, $f_{\text{lat}} = 42.41$ Hz, $f_{\text{yaw}} = 53.49$ Hz, $f_{\text{windup}} = 58.95$ Hz
$\zeta_{\text{long}} = 0.056$, $\zeta_{\text{lat}} = 0.037$, $\zeta_{\text{yaw}} = 0.0070$, $\zeta_{\text{windup}} = 0.050$
$q_{bvx} = 0.364$, $q_{bv\theta} = 0.065$

[contact_patch]
$q_{ra1} = 0.671$, $q_{ra2} = 0.733$, $q_{rb1} = 1.059$, $q_{rb2} = -1.1878$
$p_{ls} = 0.8335$, $p_{ae} = 1.471$, $p_{be} = 0.9622$, $c_e = 1.5174$

[longitudinal_coefficients]
$p_{Cx1} = 1.579$, $p_{Dx1} = 1.0422$, $p_{Dx2} = -0.08285$, $p_{Dx3} = 0$
$p_{Ex1} = 0.11113$, $p_{Ex2} = 0.3143$, $p_{Ex3} = 0$, $p_{Ex4} = 0.001719$
$p_{Kx1} = 21.687$, $p_{Kx2} = 13.728$, $p_{Kx3} = -0.4098$
$p_{Hx1} = 2.1615\text{e-}4$, $p_{Hx2} = 0.0011598$, $p_{Vx1} = 2.0283\text{e-}5$, $p_{Vx2} = 1.0568\text{e-}4$
$p_{px1} = -0.3485$, $p_{px2} = 0.37824$, $p_{px3} = -0.09603$, $p_{px4} = 0.06518$
$r_{Bx1} = 13.046$, $r_{Bx2} = 9.718$, $r_{Bx3} = 0$, $r_{Cx1} = 0.9995$, $r_{Ex1} = -0.4403$, $r_{Ex2} = -0.4663$,
$r_{Hx1} = -9.968\text{e-}5$

[overturning_coefficients]
$q_{sx1} = -0.007764$, $q_{sx2} = 1.1915$, $q_{sx3} = 0.013948$, $q_{sx4} = 4.912$, $q_{sx5} = 1.02$
$q_{sx6} = 22.83$, $q_{sx7} = 0.7104$, $q_{sx8} = -0.023393$, $q_{sx9} = 0.6581$, $q_{sx10} = 0.2824$
$q_{sx11} = 5.349$, $q_{sx12} = 0$, $q_{sx13} = 0$, $q_{sx14} = 0$, $p_{pmx1} = 0$

[lateral_coefficients]
$p_{Cy1} = 1.338$, $p_{Dy1} = 0.8785$, $p_{Dy2} = -0.06452$, $p_{Dy3} = 0$
$p_{Ey1} = -0.8057$, $p_{Ey2} = -0.6046$, $p_{Ey3} = 0.09854$, $p_{Ey4} = -6.697$, $p_{Ey5} = 0$
$p_{Ky1} = -15.324$, $p_{Ky2} = 1.715$, $p_{Ky3} = 0.3695$, $p_{Ky4} = 2.0005$, $p_{Ky5} = 0$, $p_{Ky6} = -0.8987$,
$p_{Ky7} = -0.23303$
$p_{Hy1} = -0.001806$, $p_{Hy2} = 0.00352$, $p_{Vy1} = -0.00661$, $p_{Vy2} = 0.03592$, $p_{Vy3} = -0.162$,
$p_{Vy4} = -0.4864$
$p_{py1} = -0.6255$, $p_{py2} = -0.06523$, $p_{py3} = -0.16666$, $p_{py4} = 0.2811$, $p_{py5} = 0$
$r_{By1} = 10.622$, $r_{By2} = 7.82$, $r_{By3} = 0.002037$, $r_{By4} = 0$, $r_{Cy1} = 1.0587$
$r_{Ey1} = 0.3148$, $r_{Ey2} = 0.004867$, $r_{Hy1} = 0.009472$, $r_{Hy2} = 0.009754$
$r_{Vy1} = 0.05187$, $r_{Vy2} = 4.853\text{e-}4$, $r_{Vy3} = 0$, $r_{Vy4} = 94.63$, $r_{Vy5} = 1.8914$, $r_{Vy6} = 23.8$

TABLE A3.1 TNO MF-Tire/MF-Swift 6.1 Tire Model Parameters—Cont'd

Tire Designation: 205/60R15 91 V
[rolling_coefficients] $q_{sy1} = 0.00702$, $q_{sy2} = 0$, $q_{sy3} = 0.001515$, $q_{sy4} = 8.514\text{e-}5$, $q_{sy5} = 0$ $q_{sy6} = 0$, $q_{sy7} = 0.9008$, $q_{sy8} = -0.4089$
[aligning_coefficients] $q_{Bz1} = 12.035$, $q_{Bz2} = -1.33$, $q_{Bz3} = 0$, $q_{Bz4} = 0.176$, $q_{Bz5} = -0.14853$, $q_{Bz9} = 34.5$, $q_{Bz10} = 0$ $q_{Cz1} = 1.2923$, $q_{Dz1} = 0.09068$, $q_{Dz2} = -0.00565$, $q_{Dz3} = 0.3778$, $q_{Dz4} = 0$, $q_{Dz6} = 0.0017015$ $q_{Dz7} = -0.002091$, $q_{Dz8} = -0.1428$, $q_{Dz9} = 0.00915$, $q_{Dz10} = 0$, $q_{Dz11} = 0$ $q_{Ez1} = -1.7924$, $q_{Ez2} = 0.8975$, $q_{Ez3} = 0$, $q_{Ez4} = 0.2895$, $q_{Ez5} = -0.6786$ $q_{Hz1} = 0.0014333$, $q_{Hz2} = 0.0024087$, $q_{Hz3} = 0.24973$, $q_{Hz4} = -0.21205$ $p_{pz1} = -0.4408$, $p_{pz2} = 0$ $s_{sz1} = 0.00918$, $s_{sz2} = 0.03869$, $s_{sz3} = 0$, $s_{sz4} = 0$
[turnslip_coefficients] $p_{Dx\varphi1} = 0.4$, $p_{Dx\varphi2} = 0$, $p_{Dx\varphi3} = 0$ $p_{Ky\varphi1} = 1$, $p_{Dy\varphi1} = 0.4$, $p_{Dy\varphi2} = 0$, $p_{Dy\varphi3} = 0$, $p_{Dy\varphi4} = 0$ $p_{Hy\varphi1} = 1$, $p_{Hy\varphi2} = 0.15$, $p_{Hy\varphi3} = 0$, $p_{Hy\varphi4} = -4$ $p_{E\gamma\varphi1} = 0.5$, $p_{E\gamma\varphi2} = 0$ $q_{Dt\varphi1} = 10$, $q_{Cr\varphi1} = 0.2$, $q_{Cr\varphi2} = 0.1$, $q_{Br\varphi1} = 0.1$, $q_{Dr\varphi1} = 1$

1. Constants

As can be seen from Table A3.1, many parameters of the tire model are non-dimensional. This is achieved by introducing four reference parameters: r_o, F_{zo}, V_o, and p_{io}. Parameter r_o represents the unloaded tire radius of the non-rolling tire. Parameter F_{zo} denotes the nominal load on the tire. It does not exactly have to match the actual load of the tire, but it should be in the same range. This ensures that no extreme values for the *Magic Formula* parameters will be required, which makes parameter identification faster and more robust. A typical value would be 4000 N for a passenger car tire. Parameter V_o represents a reference velocity; it is used to make parameters governing velocity-dependent effects dimensionless, e.g. rolling resistance, tire centrifugal growth, and velocity dependent changes in stiffnesses. Normally, V_o is set to the velocity at which the Force and Moment testing is done – so typically 60 km/h or 16.7 m/s. The nominal inflation pressure p_{i0} is required in the description of inflation pressure-dependent effects. If the tire is evaluated for a single tire pressure, p_{io} should be set to this value. If a more elaborate testing program is done at different tire pressures, e.g. p_{io}–0.5 bar, p_{io}, and $p_{io} + 0.5$ bar, then the tire pressure p_i in the simulation model can take any value within this range; otherwise $p_i = p_{io}$.

Please note that r_o, F_{zo}, V_o, and p_{io} should be selected with care before starting the parameter identification process and should absolutely be kept unchanged afterward. Changing them would require completely redoing the identification process!

2. Force and moment testing

The *Magic Formula* parameters are identified using Force and Moment tests. These tests can be executed on the road with a tire test trailer or in a lab using a flat-track tire tester, (cf. Chapter 12). In Table A3.1, the *Magic Formula* parameters start with [longitudinal_coefficients] up to [aligning_coefficients]. The parameters regarding turn slip, identified with [turnslip_coefficients], also belong to the *Magic Formula*, but work is still ongoing to define a suitable test and identification procedure.

Some points of attention:

Velocity dependency

Note that the contribution of the forward velocity V_x is present in the rolling resistance formula (9.231):

$$f_r = q_{sy1} + q_{sy3}|V_x/V_o| + q_{sy4}(V_x/V_o)^4 \tag{9.231}$$

that is used in connection with Eqns (9.230, 9.236). Of course, in cases such as moving on wet roads, the friction coefficient may be formulated as functions of the speed, cf. Eqn (4.E23).

Symmetric tire behavior

The measured tire characteristics may be not entirely symmetric, for example $F_y(\alpha,\gamma) \neq -F_y(-\alpha,-\gamma)$. This can be caused the tire characteristics conicity and ply steer or inaccuracies in the measurements. In some cases, it is preferable to eliminate these offsets and asymmetry and have a completely symmetric tire in the simulation environment. In that case the following parameters should be set zero and kept zero in the identification process: r_{Hx1}, q_{sx1}, p_{Ey3}, p_{Hy1}, p_{Hy2}, p_{Vy1}, p_{Vy2}, r_{By3}, r_{Vy1}, r_{Vy2}, q_{Bz4}, q_{Dz6}, q_{Dz7}, q_{Ez4}, q_{Hz1},q_{Hz2}, s_{sz1}, and q_{Dz3}.

Incomplete measurement set

The Force and Moment testing can be divided into three different types of tests:

- Kappa sweep: variation of the longitudinal slip κ, while keeping the side slip angle α equal to zero.
- Alpha sweep: variation of the slip angle α for a freely rolling tire, ($\kappa = 0$).
- Combined slip: variation of the longitudinal slip κ for non-zero values of the side slip angle α.

The structure of the *Magic Formula* is such that different parts of the formulas are responsible for modeling different aspects of the tire behavior.

All parameters in the [longitudinal_coefficients] section starting with a *p* are determined by kappa sweeps, combined slip is modeled by coefficients starting with an *r* and *s*, etc.

A situation, which may occur in practice, is that only alpha sweeps are available but no measurements including longitudinal slip κ variations. Then it is still possible to combine the parameters of an existing tire with the newly identified *Magic Formula* parameters for the alpha sweeps to obtain a new tire parameter set. This set then combines the longitudinal and combined slip parameters of the existing tire with the lateral behavior based on the latest measurements. Practical experience has shown that the parameters of the combined slip weighting functions are relatively constant for various tires.

It is clear that the approach described above is not ideal, but may be necessary due to a restricted number of measurements being available. Once combining different tire parameter sets, it is in any case important to visually check the resulting tire characteristics. Another consideration is the application of the tire model: e.g. if only straight line simulations are done, the accuracy of the lateral tire behavior may be less important.

No measurement data at all

In some cases no Force and Moment data are available at all, e.g. when considering the tires of a fork lift truck, agricultural vehicle, etc. Still, wanting to simulate such a vehicle, an estimate for some *Magic Formula* parameters can be made and it can be improved when measurement data become available.

To start, all *Magic Formula* parameters are set to zero, with the following exceptions: $p_{Ky2} = 2$, $q_{sy7} = 1$, and $q_{sy8} = 1$. For the combined slip weighting functions, the following values are suggested: $r_{bx1} = 8.3$, $r_{Bx2} = 5$, $r_{Cx1} = 0.9$, $r_{By1} = 4.9$, $r_{By2} = 2.2$, and $r_{Cy1} = 1$.

The friction coefficient in longitudinal and lateral directions at the nominal vertical tire force is controlled by p_{Dx1} and p_{Dy1}, respectively. Generally, the friction coefficient for highly loaded tires is below 1, possibly 0.8 on a dry surface, whereas for high performance tires used on motorcycles or on racing cars the friction coefficient may become 1.5 or even 2 in extreme cases. If desired, load dependency of the friction coefficient can be introduced by adapting p_{Dx2} and p_{Dy2}. Note that generally $p_{Dy2} < p_{Dx2}$ and that they normally are below zero (typically between -0.1 and 0). If different values are used for p_{Dx2} and p_{Dy2}, it is good to ensure that, at a vertical load tending to zero, the longitudinal and lateral friction coefficients become equal to each other.

The longitudinal slip stiffness is for many tires (almost) linearly dependent on the vertical force. This is controlled by parameter p_{Kx1}; typically, the value of this parameter is in the range of 14 to 18, although it may be much higher for racing tires. The dependency of the cornering stiffness on the vertical tire force is less linear. The shape is controlled by p_{Ky1} and p_{Ky2} as shown in the left (picture) of Figure 4.12. The maximum cornering stiffness normally does not occur at the nominal vertical force but is generally higher, so p_{Ky2} may be in the range 1.5 to 3. The maximum value of the cornering stiffness is controlled by p_{Ky1} for which no narrow range can be given: expect values between 10 and 20 (or higher for racing tires). In the TNO MF-Tire model, the ISO sign convention is used and then p_{Ky1} should be negative.

Finally, the shape of the longitudinal slip curve is determined by parameters p_{Cx1} and p_{Ex1} and the same applies to the lateral direction: parameters p_{Cy1} and p_{Ey1} control the shape of the lateral force as a function of the side slip angle. Taking $p_{Cx1} = 1.6$ and $p_{Cy1} = 1.3$ and leaving p_{Ex1} and p_{Ey1} equal to zero should be a fair starting point. The effect of modifications to p_{Ex1} and p_{Ey1} is illustrated by Figure 4.10: an increasing negative E value will make the resulting characteristic more 'peaky'. In any case, $p_{Cx1} \geq 1$, $p_{Cy1} \geq 1$, $p_{Ex1} \leq 1$ and $p_{Ey1} \leq 1$.

3. Loaded radius/effective rolling radius

Figure A3.1 illustrates the various tire radii: the free tire radius of the rotating tire r_Ω, the loaded tire radius r_l and effective rolling radius r_e.

First, centrifugal growth of the free tire radius r_Ω is calculated using the following formula:

$$r_\Omega = r_o\left(q_{reo} + q_{V1}\left(\frac{r_o\Omega}{V_o}\right)^2\right) \tag{A3.1}$$

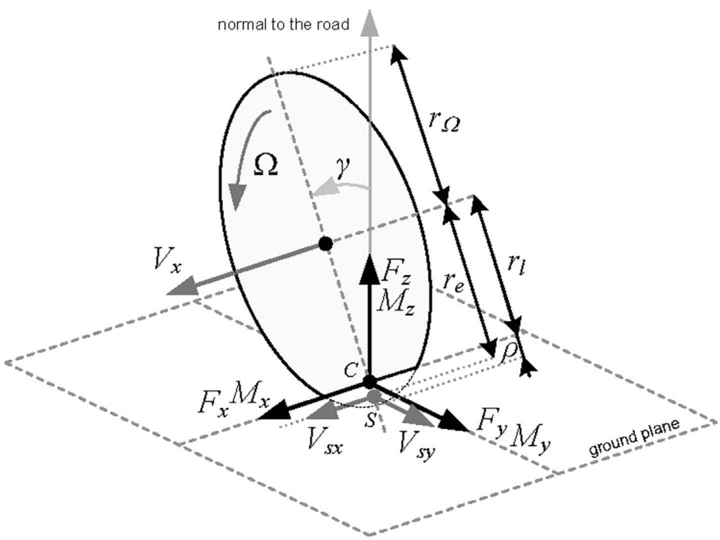

FIGURE A3.1 ISO sign convention for the tire forces and moments and definition of tire radii.

The parameter q_{re0} is introduced to adapt the free unloaded radius to the measurements. The tire normal deflection ρ is the difference between the free tire radius of the rotating tire r_Ω and the loaded tire radius r_l (cf. Eqn (9.218)):

$$\rho = \max(r_\Omega - r_l, 0) \tag{A3.2}$$

The vertical tire force F_z is then calculated using the following formula:

$$\begin{aligned} F_z = & \left\{1 + q_{V2}|\Omega|\frac{r_o}{V_o} - \left(q_{Fcx1}\frac{F_x}{F_{zo}}\right)^2 - \left(q_{Fcy1}\frac{F_y}{F_{zo}}\right)^2\right\} \\ & \cdot F_{zo}\left(q_{Fz1}\frac{\rho}{r_o} + q_{Fz2}\frac{\rho^2}{r_o^2}\right)(1 + p_{Fz1}\mathrm{d}p_i) \end{aligned} \tag{A3.3}$$

Various effects are included in this expression: a stiffness increase with velocity (q_{v2}), vertical sinking due to longitudinal and lateral forces (q_{Fcx1} and q_{Fcy1}), a quadratic force deflection characteristic (q_{Fz1} *and* q_{Fz2}) and the influence of the tire inflation pressure (p_{Fz1}). The vertical stiffness c_{zo} at the nominal vertical load, nominal inflation pressure, no tangential forces, and zero forward velocity can be calculated as

$$c_{zo} = \frac{F_{zo}}{r_o}\left(q_{Fz1} + 2q_{Fz2}\frac{\rho_o}{r_o}\right) = \frac{F_{zo}}{r_o}\sqrt{q_{Fz1}^2 + 4q_{Fz2}} \tag{A3.4a}$$

The derivation of the last expression is given in section 10 at the end of this Appendix. In the expressions for the effective rolling radius and contact patch dimensions, the vertical stiffness adapted for tire inflation pressure is used:

$$c_z = c_{zo}(1 + p_{Fz1}\mathrm{d}p_i) \tag{A3.5}$$

The effective rolling radius, similar to (9.232), is calculated as

$$r_e = r_\Omega - \frac{F_{zo}}{c_z}\left\{F_{\mathrm{reff}}\frac{F_z}{F_{zo}} + D_{\mathrm{reff}}\arctan\left(B_{\mathrm{reff}}\frac{F_z}{F_{zo}}\right)\right\} \tag{A3.6}$$

The parameters D_{reff}, etc., can be found in Table A3.1.

The measurement data for assessing the loaded and the effective rolling radius typically consist of values for r_l, r_e, V, F_x, F_y, and F_z carried out for a number of different vertical loads, forward velocities, and possibly longitudinal and/or lateral forces. Based on the relation $V = \Omega r_e$, it is sufficient to specify two out of three variables: forward velocity V, angular velocity Ω, and effective rolling radius r_e. The data for F_x and F_y can be considered optional for passenger car tires, but generally should be included for racing tires. Fitting of the parameters is generally done in two steps. In order to obtain maximum accuracy for the loaded radius, the Eqns (A3.1) and (A3.3) are fitted first. In a second step, the coefficients for the effective rolling radius, as given by Eqn (A3.6), are determined.

When only a tire radius r_o and vertical stiffness c_{zo} are available, many parameters can be set to zero: q_{V1}, q_{V2}, q_{Fcx1}, q_{Fcy1}, q_{Fz2}, and p_{Fz1} while q_{reo} is set to one. In this case, the parameter q_{Fz1} can be calculated easily using eqn (A3.4) since $q_{Fz2} = 0$. The parameters in the expression for the effective rolling radius (B_{reff}, D_{reff}, and F_{reff}) may be set to zero, but for a radial tire the following values are suggested: $B_{reff} = 8$, $D_{reff} = 0.24$, and $F_{reff} = 0.01$. For a bias ply tire: $B_{reff} = 0$, $D_{reff} = 0$, and $F_{reff} = 1/3$. To include the effect of a changing tire inflation pressure on the tire vertical stiffness, the parameter p_{Fz1} needs to be non-zero; the suggested value would be in the range of 0.7 to 0.9.

4. Contact patch dimensions

The following formulas are used for the contact patch dimensions. The length a represents half of the contact length and b half of the width of the contact patch:

$$a = r_o\left(q_{ra2}\frac{F_z}{c_z r_o} + q_{ra1}\sqrt{\frac{F_z}{c_z r_o}}\right) \approx r_o\left(q_{ra2}\frac{\rho}{r_o} + q_{ra1}\sqrt{\frac{\rho}{r_o}}\right) \tag{A3.7}$$

$$b = w\left(q_{rb2}\frac{F_z}{c_z r_o} + q_{rb1}\left(\frac{F_z}{c_z r_o}\right)^{\frac{1}{3}}\right) \approx w\left(q_{rb2}\frac{\rho}{r_o} + q_{rb1}\left(\frac{\rho}{r_o}\right)^{\frac{1}{3}}\right) \tag{A3.8}$$

Consequently, measurement data should provide half the contact length and half the contact width as a function of the vertical load F_z. Actually, the contact length is not so much directly dependent on the vertical tire force, but is more a geometrical property and dependent on the vertical tire deflection ρ, as indicated in the right-hand side part of Eqns (A3.7) and (A3.8). If no measurement data are available, based on the work of Besselink (2000) the following values are suggested: $q_{ra2} = 0.35$ and $q_{ra1} = 0.79$.

5. Overall longitudinal and lateral stiffness, relaxation lengths

Relaxation behavior of the tire can be modeled using a first order differential equation and an explicit expression for the relaxation length as a function of the vertical load. When rigid ring dynamics are included on the other hand, the relaxation lengths become a function of the longitudinal and lateral stiffness of the tire, respectively. As the TNO MF-Tire/MF-Swift 6.1 tire model is able to handle both conditions, the relaxation length is included in the model using explicit expressions for the non-rolling longitudinal and lateral stiffness:

$$\sigma_x = \frac{C_{F\kappa}}{c_x} \tag{A3.9}$$

$$\sigma_y = \frac{C_{F\alpha}}{c_y}$$

where σ_x is the longitudinal relaxation length, $C_{F\kappa}$ the longitudinal slip stiffness of the tire, c_x the nonrolling longitudinal stiffness at ground level, σ_y the lateral relaxation length, $C_{F\alpha}$ the cornering stiffness of the tire, c_y the nonrolling lateral stiffness at ground level.

The stiffnesses are made dependent on both the vertical force df_z and the inflation pressure increment dp_i:

$$c_x = c_{xo}(\,1 + p_{cfx1}df_z + p_{cfx1}df_z^2)(1 + p_{cfx3}dp_i) \tag{A3.10}$$

$$c_y = c_{yo}(\,1 + p_{cfy1}df_z + p_{cfy1}df_z^2)(1 + p_{cfy3}dp_i) \tag{A3.11}$$

where c_{xo} and c_{yo} are the longitudinal and lateral stiffness of the tire at the nominal vertical force and inflation pressure.

In principle, the stiffness c_{xo} and c_{yo} may be measured on a non-rolling tire, but in general the relaxation length based on the non-rolling lateral stiffness is too short compared to the measurements on a rolling tire. The preferred approach therefore is to measure the cornering stiffness and lateral relaxation length in a transient test for a number of different inflation pressures and vertical loads. Subsequently, the overall lateral stiffness equation can be fitted to these measurement points accordingly.

In case no transient tests are available, the non-rolling stiffnesses can still be used to model relaxation behavior, albeit with a reduced accuracy. If no non-rolling static stiffness tests are available, a first, crude rule of thumb is that the lateral stiffness c_{yo} equals half of the vertical stiffness c_{zo} and the longitudinal stiffness c_{xo} is twice the vertical stiffness. To include the effect of the inflation pressure on these stiffnesses, the parameters p_{cfx3} and p_{cfy3} can be set to 0.2 and 0.5, respectively, as a first estimate.

6. Tire inertia

When rigid ring dynamics are employed, the tire is not considered as a single rigid body any more. A part of the tire near the rim is assumed to be rigid and fixed to the rim. The other part that represents the belt is considered to move as a rigid ring. Consequently, the total tire mass has to be divided and a distribution has to be made over the inertia of the ring and the inertia of the part rigidly attached to the rim. The latter part is further regarded as a part of the wheel body. An estimate of this division can be made based on past experience or on a detailed weight breakdown provided by the tire manufacturer. The following rough initial estimate is suggested:

75% of the tire mass is assigned to the tire belt
85% of the tire moments of inertia is assigned to the tire belt

Tentatively, the contact patch body is considered as an additional small mass.

7. Carcass compliances

The rigid belt ring is elastically suspended with respect to the rim in all directions. So, various stiffnesses are associated with these motions: c_{bx}, c_{by}, $c_{b\theta}$, and $c_{b\gamma}$ as is illustrated in Figure A3.2.

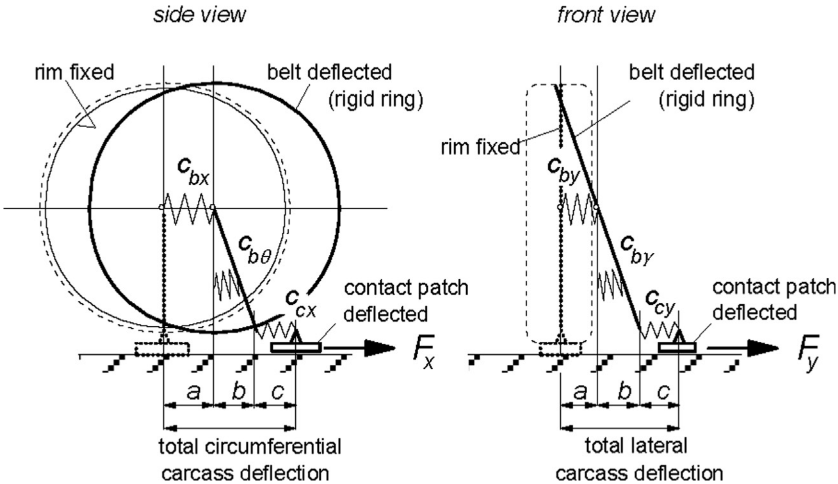

FIGURE A3.2 Springs connecting rigid ring to the rim and contact patch to the rigid ring.

In the tire property file, the choice has been made to allow the user to specify the eigenfrequencies f [Hz] of the belt for a tire not in contact with the ground and the rim fixed. The corresponding stiffnesses then become

$$c_{bx} = c_{bz} = 4\pi^2 m_{\text{belt}} f_{\text{long}}^2 \tag{A3.12}$$

$$c_{by} = 4\pi^2 m_{\text{belt}} f_{\text{lat}}^2 \tag{A3.13}$$

$$c_{b\theta} = 4\pi^2 I_{yy,\text{belt}} f_{\text{windup}}^2 \tag{A3.14}$$

$$c_{b\gamma} = c_{b\psi} = 4\pi^2 I_{zz,\text{belt}} f_{\text{yaw}}^2 \tag{A3.15}$$

where f_{long} equals the eigenfrequency (in Hz) of the longitudinal/vertical motion of the tire belt, f_{lat} equals the eigenfrequency of the lateral motion, f_{windup} the eigenfrequency of the in-plane torsional mode, and f_{yaw} the eigenfrequency of the yaw (and roll) mode of the belt. Obviously, m_{belt} refers to the mass of the belt and $I_{yy,\text{belt}}$ and $I_{zz,\text{belt}}$ to the belt moment of inertia about the y- and z-axes. The natural frequencies are assessed for a free unloaded tire mounted on a rim fixed with respect to space.

As can be seen from Figure A3.2, the deflection of the contact patch is the result of the deflection of a number of successive springs. The expressions for the overall longitudinal and lateral stiffness have already been given in step (5). Therefore, the stiffness of the residual springs c_{cx} and c_{cy} should be chosen such that the overall stiffnesses become correct. The expression for the overall longitudinal stiffness reads

$$\frac{1}{c_x} = \frac{1}{c_{bx}} + \frac{r_l^2}{c_{b\theta}} + \frac{1}{c_{cx}} + \frac{a}{C_{F\kappa}} \tag{A3.16}$$

In the lateral direction, the overall stiffness becomes

$$\frac{1}{c_y} = \frac{1}{c_{by}} + \frac{r_l^2}{c_{b\gamma}} + \frac{1}{c_{cy}} + \frac{a}{C_{F\alpha}} \tag{A3.17}$$

Making sure that Eqn (A3.16) and (A3.17) hold for all vertical loads and inflation pressures is not trivial. In any case, it is clear that from a physical point of view the residual springs never should get a negative stiffness.

If no measurement data are available to identify the eigenfrequencies of the tire belt, another approach can be followed to determine the stiffness of the various springs. Based on past measurement results, the contribution of the various springs on the overall carcass deflection at ground level has been identified, see Table A3.2. Here it is assumed that a longitudinal or lateral force is applied at ground level and that the rim is held fixed, cf. Figure A3.2.

Table A3.2 shows the relative contributions *a*, *b*, and *c* that have been assessed for three different tires. Based on these data, it may be concluded that although the compliance values themselves are different, the relative contributions to the overall carcass deflection are fairly constant. Since in step (5) the overall longitudinal and lateral carcass stiffnesses have been determined, it is now possible to assess approximate individual stiffness values using the suggested 'rule of thumb'.

Additional measurement data (e.g. yaw stiffness or *FEM* model results) may also be used to enhance the estimates or to gain additional confidence in the stiffness/deflection distribution.

TABLE A3.2 Distribution of Longitudinal and Lateral Carcass Compliance Components

Longitudinal at Ground Level	Tire 1	Tire 2	Tire 3	Rule of Thumb
Rigid ring translation (a)	27%	28%	31%	30%
Rigid ring rotation (b)	63%	62%	60%	60%
Contact patch translation (c)	10%	10%	9%	10%
Lateral at Ground Level	**Tire 1**	**Tire 2**	**Tire 3**	**Rule of Thumb**
Rigid ring translation (a)	34%	25%	27%	25%
Rigid ring rotation (b)	62%	56%	55%	55%
Contact patch translation (c)	4%	19%	18%	20%

8. Carcass damping

Generally, the exact amount of damping of the tire is very difficult to assess experimentally. For instance, it is observed that a large difference in vertical damping exists between a tire that stands still and a tire that rolls: under rolling conditions the apparent damping may be a factor 10 smaller compared to the damping of a tire standing still, also cf. Jianmin et al. (2001). A simple model with finite contact length and provided with radial dry friction dampers (Pacejka 1981a) may explain this phenomenon.

Based on experience, the following guideline may be provided: when the tire is not in contact with the ground (and the rim is fixed) the damping will be relatively low. Typical values of the damping coefficients lie in the range of 1 to 6% of the corresponding critical damping coefficients. Generally, the modes that contain a large translational component are more heavily damped than the modes with a large rotational component.

In the tire property file, the dimensionless damping coefficient for the four vibration modes is specified: ζ_{long}, ζ_{lat}, ζ_{yaw}, and ζ_{windup}. Given the observations above, their values should normally be in the range of 0.01 to 0.06.

9. Enveloping

The enveloping model uses elliptical cams that approximate the tire contour at the leading and trailing parts of the contact point. The shape of the ellipse is described by

$$\left(\frac{x_e}{a_e}\right)^{c_e} + \left(\frac{z_e}{b_e}\right)^{c_e} = 1 \tag{A3.18}$$

with $a_e = p_{ae}r_o$ and $b = p_{be}r_o$. The parameter p_{ae} defines the length of the ellipse and p_{be} the height of the ellipse. As both parameters are dimensionless, the size of the ellipse scales linearly with the tire radius r_o, which is plausible from a physical point of view. When no measurements are available, the following parameters could be used as a starting point: $p_{ae} = 1$, $p_{be} = 1$, and $c_e = 1.8$.

The distance between the ellipses is given by l_s. This distance depends on the contact length $2a$. The following relation is used:

$$l_s = 2p_{ls}a \tag{A3.19}$$

If no measurement data are available, the suggested value for p_{ls} is 0.8.

10. Derivation of expression for vertical stiffness

Starting with (A3.3) for the vertical force and eliminating all velocity, force, and inflation pressure dependent effects, results in

$$F_z = F_{zo}\left(q_{Fz1}\frac{\rho}{r_o} + q_{Fz2}\frac{\rho^2}{r_o^2}\right) \tag{A3.20}$$

When the vertical force is equal to the nominal force, $(F_z = F_{zo})$ the next equation holds for the vertical tire deflection:

$$q_{Fz2}\frac{\rho^2}{r_o^2} + q_{Fz1}\frac{\rho}{r_o} - 1 = 0 \tag{A3.21}$$

The possible solutions to this equation are

$$\frac{\rho}{r_o} = \frac{-q_{Fz1} \pm \sqrt{q_{Fz1}^2 + 4q_{Fz2}}}{2q_{Fz2}} \tag{A3.22}$$

The vertical stiffness derived from (A3.20) is given by

$$\frac{\partial F_z}{\partial \rho} = F_{zo}\left(\frac{q_{Fz1}}{r_o} + \frac{2q_{Fz2}}{r_o}\left(\frac{\rho}{r_o}\right)\right) \tag{A3.23}$$

The vertical stiffness at the nominal vertical force F_{zo} can be obtained by substituting (A3.22) in (A3.23):

$$c_{zo} = F_{zo}\left(\frac{q_{Fz1}}{r_o} + \frac{2q_{Fz2}}{r_o}\left(\frac{-q_{Fz1} \pm \sqrt{q_{Fz1}^2 + 4q_{Fz2}}}{2q_{Fz2}}\right)\right) \tag{A3.24}$$

After simplification, this results in the second expression of (A3.4b), as a positive stiffness is the only physical solution:

$$c_{zo} = \frac{F_{zo}}{r_o}\sqrt{q_{Fz1}^2 + 4q_{Fz2}} \tag{A3.4b}$$

This expression is of interest because at given c_{zo} and q_{Fz2} (cf. the tire property file shown in Table A3.1) q_{Fz1} and with this the vertical force (A3.3) can be calculated.